J. Membrane Biol. 156, 141–148 (1997)

The Journal of
Membrane
Biology

Structure-Function Relationship of the Ion Channel Formed by Diphtheria Toxin in Vero Cell Membranes

M. Lanzrein,[1]* P.Ø. Falnes,[1] O. Sand,[2] S. Olsnes[1]

[1]Institute for Cancer Research, The Norwegian Radium Hospital, Montebello, 0310 Oslo, Norway
[2]Department of Biology, University of Oslo, PO Box 1051, Blindern, 0316 Oslo, Norway

Received: 20 June 1996/Revised: 8 November 1996

Abstract. Diphtheria toxin (DT) forms cation selective channels at low pH in cell membranes and planar bilayers. The channels formed by wild-type full length toxin (DT-AB), wild-type fragment B (DT-B) and mutants of DT-B were studied in the plasma membrane of Vero cells using the patch-clamp technique. The mutations concerned certain negatively charged amino acids within the channel-forming transmembrane domain (T-domain). These residues might interact electrostatically with cations flowing through the channel, and were therefore exchanged for uncharged amino acids or lysine. The increase in whole-cell conductance induced by toxin, Δg_m, was initially determined. DT-AB induced a ~10-fold lower Δg_m than DT-B. The mutations DT-B E327Q, DT-B D352N and DT-B E362K did not affect Δg_m, whereas DT-B D295K, DT-B D352K and DT-B D318K drastically reduced Δg_m. Single channel analysis of DT-B, DT-AB, DT-B D295K, DT-B D318K and DT-B E362K was then performed in outside-out patches. No differences were found for the single-channel conductances, but the mutants varied in their gating characteristics. DT-B D295K exhibited only a very transient channel activity. DT-AB as well as DT-B D318K displayed significantly lower open probability and mean dwell times than DT-B. Hence, the lower channel forming efficiency of DT-AB and DT-B D318K as compared to DT-B is reflected on the molecular level by their tendency to spend more time in the closed position and the fast flickering mode.

Altogether, the present work shows that replacements of single amino acids distributed throughout a large part of the transmembrane domain (T-domain) strongly affect the overall channel activity expressed as Δg_m and the gating kinetics of single channels. This indicates clearly that the channel activity observed in DT-exposed Vero cells at low pH is inherent to DT itself and not due to DT-activation of an endogenous channel.

Key words: Diphtheria toxin — Membrane translocation — Ion channel — Site directed mutagenesis — Patch clamp

Introduction

Many bacterial protein toxins, such as diphtheria toxin, pseudomonas exotoxin A, anthrax toxin, tetanus toxin and cholera toxin, are composed of an enzymatic moiety (A-domain) which is able to enter target cells by help of a second moiety (B-domain), which binds to cellular receptors and facilitates membrane translocation of the A-domain. This family of toxins is therefore often referred to as A-B-toxins [21]. Diphtheria toxin (DT) is one of the most potent bacterial toxins, entry of only one molecule is sufficient to kill a cell [31]. The toxin is secreted from *Corynebacterium diphtheriae* as a polypeptide of 58 kDa [11], which is proteolytically cleaved in an arginine-rich region to yield fragments A (21 kDa) and B (37 kDa), held together by a disulfide bridge [23]. Fragment A is the enzymatically active part that ADP-ribosylates elongation factor 2, thereby inhibiting protein synthesis [6]. Fragment B binds to the cellular receptor and inserts into the membrane when it meets the low pH in endosomes, thereby enabling fragment A to cross the barrier of the endosomal membrane and enter the cytosol.

The crystal structure of DT [2, 3, 5] revealed that fragment B contains two structural domains (Fig. 1).

* *Present address:* Division of Biology 156-29, California Institute of Technology, Pasadena, CA 91125.

Correspondence to: S. Olsnes

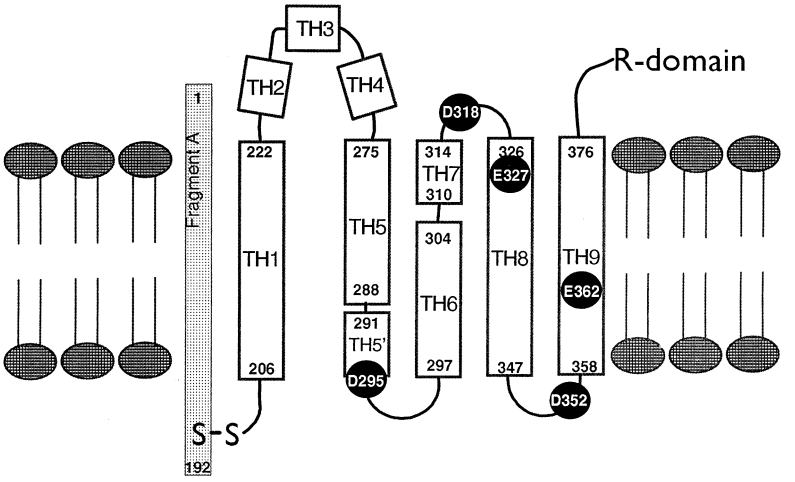

Fig. 1. Schematic drawing showing a putative topology of the membrane-inserted diphtheria toxin. Mutated amino acids are highlighted with black spheres. TH1-TH9: Alphahelical stretches of the translocation-domain according to [2]; R-domain: receptor-binding domain (modified after [20]). The top represents the outside of the membrane, the bottom the cytosolic side.

The R-domain, which confers receptor binding, consists of a flattened β-barrel in a jelly-roll-like topology, reminiscent of variable domains in immunoglobulins. The T-domain is formed by ten alpha helical domains (TH1-TH9, TH5′). These helices are arranged in three layers, with the long apolar helices TH8 and TH9 in the center, flanked by TH5-TH7 which also contain hydrophobic residues, and the hydrophilic helices TH1-TH3. The hydrophobic helical hairpins TH8/TH9 and TH5-TH7 are believed to insert into the membrane at low pH.

DT, like many other toxins from the A-B family, inserts into artificial membranes and forms an ion channel [8, 13]. This channel has been characterized to a large extent and its topology in the membrane bilayer was determined [17, 18, 27]. It was shown that the helical hairpin TH8/TH9 is sufficient to form a channel with a similar signature as the wild-type toxin channel [27]. Thus, it was concluded that TH8/TH9 is the channel-forming region. TL5, the loop connecting TH8/TH9 contains two negatively charged aspartates, D349 and D352. These residues were titratable only from the *trans* side (the side opposite to where the toxin was added) [18]. Exchanging D352 with lysine significantly reduced single channel conductance, consistent with D352 interacting electrostatically with ions in the channel at the *trans* side. Introducing charges with sulfhydryl-specific reagents on cysteines substituted at positions 350–352 confirmed this notion [19]. Single-channel conductance was also altered when E362 was mutated, but this residue was titratable from both the *trans* and *cis* sides, indicating that this residue is projecting into the lumen of the channel [17].

In cell membranes, DT induced cation permeability upon exposure to low pH [22, 25]. Voltage clamped Vero cells exhibited a large decrease in input resistance and depolarized in response to DT and low pH [9]. Furthermore, single-channel analysis revealed a new, DT-induced channel selective for monovalent cations. The channel had a conductance of ~30 pS, which is substantially different from the conductance of ~10 pS in artificial membranes [8, 13]. The latter result can be interpreted in two ways: (i) Interaction of DT with its native receptor alters the channel properties [14]. (ii) The recordings from Vero cells did not represent the DT-channel but instead showed an endogenous channel present in Vero cells that is activated by DT. Indeed, a nonselective cation channel with similar properties as the one described in ref. 9 has been characterized in MDCK renal epithelial cells [7]. This channel is activated by Maitotoxin. Furthermore, calcium-activated, nonselective cation channels with conductances around 30 pS have been reported in renal tissue [1, 16, 24, 30]. Since Vero cells originate from renal tissue, the possibility of DT activating an endogenous, nonselective channel has to be considered. To address this issue, we have studied the channels formed by a series of mutants with single amino acid substitutions in the T-domain of DT fragment B in Vero cells. If the DT molecule is itself a constituent of the channel, and not merely an activator, such mutations are likely to have variable effects on the channel properties. The present data suggest that this is the case: three of the six mutations studied affected the whole cell conductance, Δg_m, induced by DT and two of them altered single channel gating kinetics. DT-AB and the mutants DT-B D318K and DT-B E362K had channel properties different from the ones reported in planar bilayers, indicating that the presence of the natural receptor results in a channel with a topology different from the one in artificial membranes.

Materials and Methods

Chemicals

^{35}S-Methionine was obtained from Amersham. All other chemicals were of the highest purity commercially available.

Buffers and Solutions

Dialysis buffer consisted of 140 mM NaCl, 20 mM HEPES (N-2-hydroxyethylpiperazine-N′-2-ethanesulfonic acid)/NaOH, and 2 mM $CaCl_2$, pH 7.0. Solutions used for patch-clamp experiments: Pipette solution consisted (in mM) of 120 potassium gluconate, 5 KCl, 1 $MgCl_2$, 1 EGTA, 1 ATP, 5 HEPES/KOH, pH 7.2, 1 μM $CaCl_2$. Krebs Ringer solution consisted of (in mM): 140 NaCl, 5 KCl, 2.4 $CaCl_2$ (replaced by 2.4 $BaCl_2$ for whole-cell experiments), 1.3 $MgCl_2$, 10 Glucose, 0.02% BSA, 10 HEPES/NaOH, pH 7.4. Gluconate buffer consisted of (in mM): 140 NaCl, 5 KCl, 2.4 $CaCl_2$, 1.3 $MgCl_2$, 10 glucose, 0.02% BSA, 10 Na-gluconate/HCl, pH 4.5.

Cell Culture

Cells were maintained and propagated under standard conditions (5% CO_2 in Eagle's minimal essential medium containing 10% FCS). Two days prior to the experiments the cells were seeded into 35 mm culture dishes. Vero cells have gap junctions and to facilitate recordings from single, independent cells, the seeding density was low, i.e., not exceeding 10,000 cells per dish.

Nicking of Diphtheria Toxin

DT at a concentration of 1.1 mg/ml was nicked with trypsin at 0.5 μg/ml for 30 min at 37°C. The reaction was stopped by adding 25 μg/ml of soybean trypsin inhibitor.

Patch-Clamp Recordings

Recordings were made in the whole-cell and outside-out modes [12]. Patch electrodes were produced by a two-step electrode puller (Narishige, Japan), and fire-polished. For single-channel recordings, the electrodes were coated with Sylgard. The electrode resistance was 6–15 MΩ. The electrodes were connected to standard recording equipment. The recordings were performed at room temperature at the stage of an inverted microscope. For the whole cell recordings, the holding potential was −40 mV and the membrane potential was shifted between −100 and +40 mV in 20 mV steps of 200 msec duration. The resulting current at the end of each voltage step was measured and plotted *vs.* the membrane potential. The cells were exposed to low pH by pressure ejection (~5 kPa) of gluconate buffer, pH 4.5, through a micropipette (inner tip diameter: ~2 μm) positioned 15–20 μm from the cell.

Construction of the Mutants

Construction of the plasmids encoding the mutants D295K, D318K and E362K has previously been described [10]. Plasmids encoding mutants D352K, D352N and E327Q were generously given to us by Dr. R. John Collier, Harvard Medical School, Boston, MA. The *Cla*I-*Kpn*I fragments from these plasmids were subcloned into pBD–48 [10].

In Vitro Transcription and Translation

Plasmid DNA was linearized with *Eco*RI downstream of the encoding gene and transcribed in a 20 μl reaction mixture with T3 RNA polymerase as described [15]. The mRNA was precipitated with ethanol and dissolved in 10 μl H_2O containing 10 mM dithiothreitol and 0.1 units/μl Rnasin. The translation was performed in micrococcal nuclease-treated rabbit reticulocyte lysate using 5 μl of the dissolved mRNA/100 μl of lysate. Proteins were made with lysates containing 25 μM of each of the 20 natural amino acids. The amount of translated protein in the nonlabeled lysates was estimated as previously described [28] by translating in parallel a 10 μl aliquot of the lysate in the presence of 5 μM [^{35}S]methionine. The translation mixture was dialyzed overnight against dialysis buffer to remove free methionine and reducing agent.

Results

The biochemical characteristics and the channel properties in planar bilayers of the mutants of DT used in the current work have previously been described [10, 17, 18, 26, 27]. Figure 1 shows a putative model of the topology of DT-insertion into the membrane and depicts the location of the negatively charged amino acids that were mutated. The two α-helical hairpins, TH5/TH6-TH7 and TH8/TH9 presumably insert into the membrane at low pH, and hence their connecting loops, TL3 and TL5, respectively, probably cross the membrane during insertion [2, 3, 5, 32]. Due to the energy barrier for charged residues to cross the membrane, penetration is probably facilitated at low pH by protonation of the negatively charged amino acids D295 in TL3 and E349/D352 in TL5. The mutants D295K and D352K used in this study contain a positively charged lysine instead of a low pH titratable aspartate, presumably hindering insertion and channel activity. Two other mutations E327Q and E362K were made at sites within TH8 and TH9, respectively. Finally, the aspartate at position 318, situated in TL4, the loop connecting TH7 and TH8, was exchanged with lysine. The mutants used in this study have previously been shown not to differ from DT-B in their ability to bind to cellular receptors and in their sensitivity to trypsin digestion [10, 26].

Effects of Toxin on Whole-Cell Currents

DT-B and mutants thereof were expressed *in vitro* in reticulocyte lysates. Vero cells were exposed to purified, nicked full length toxin (DT-AB) or toxin expressed *in vitro* for 20 min at 20°C. The cells were then washed and bathed in Krebs-Ringer solution containing 2.4 mM $BaCl_2$. Whole-cell recordings from clustered cells show great variability of membrane conductance, due to gap junctions between neighboring cells. Recordings were therefore restricted to single, independent cells. The membrane conductance was furthermore minimized by substitution of Ca^{2+} with the general K^+-channel blocker Ba^{2+} in the recording solution to enhance the detection sensitivity to toxin-induced conductance elevations. *I-V* curves were recorded in this solution prior to and approximately 10 sec after starting to eject gluconate-buffer, pH 4.5, directly onto the cells. Ejection of low pH buffer to toxin-exposed cells caused depolarization

and drop in input resistance, R_m. The time course of this response was not studied in detail, but it reached steady state within ~5 sec after start of the ejection. Figure 2 shows *I/V* plots for cells exposed to DT-AB, DT-B and all the mutants. From these plots Δg_m, the conductance induced by toxin, was calculated as the difference between the g_m after and before exposure to low pH. The data are summarized in Table 1. DT-B induced an 8-fold larger increase in g_m than DT-AB. This is consistent with earlier findings showing that DT-B was more effective than DT-AB in inducing $^{22}Na^+$ influx into Vero cells [29]. Three of the single amino acid substitutions in the T-domain, D352N, E327Q and E362K, did not affect the ability to increase g_m as compared to DT-B. For D318K, however, Δg_m was significantly smaller and in the same range as for DT-AB. D352K and D295K induced conductance changes of 610 pS and 270 pS, respectively. The latter effects were relatively small, albeit still significantly different from controls with ''empty'' lysate (two-tailed student's *t*-test, $P < 0.001$). The reversal potential V_{rev} of the DT-induced current was estimated for each cell from the point of intersection of the two *I/V* plots. V_{rev} was around 0–20 mV for all the channels (*data not shown*).

Analysis of Single-Channel Properties

To study the differences of the conductance change induced by DT and its mutants in molecular detail, we performed single-channel recordings with some of the toxins. Vero cells were exposed to toxin, washed and then bathed in normal Krebs-Ringer solution. Outside-out patches were then excised from cells and exposed to low pH by placing the patches into a stream of gluconate buffer from a large pipette (tip diameter ~5 μm). We have previously reported the presence of large channels probably selective for K^+ in Vero cells [9]. These channels were observed in almost all (~80%) of the outside-out patches studied. Upon exposure to low pH buffer, DT-induced single channel activity could be observed, although only in a minor part of the patches (20–30%). When channel activity was observed, it usually appeared immediately after placing the patches into the stream of gluconate buffer, pH 4.5. DT channel activity occurred in bursts, i.e., phases of strong activity were separated by long silent periods. Figure 3 shows representative recordings of single channels formed by DT-B, DT-AB, DT-B D295K, DT-B D318K and DT-B E362K during bursts at a holding potential of −80 mV. For DT-B D295K, channel activity was only rarely observed (in about 5% of the patches) and it was very transient. We did not succeed in recording any single-channel activity from cells exposed to reticulocyte lysate containing DT-B D352K.

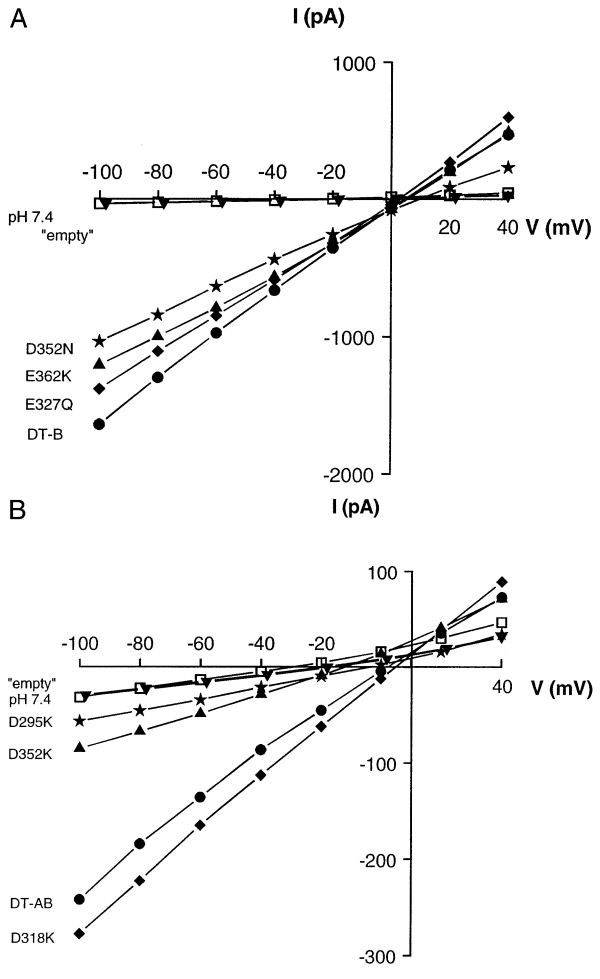

Fig. 2. *I/V* relationships from DT-exposed cells before and after ejection of low pH solution. Vero cells were incubated for 20 min at 20°C in Krebs-Ringer solution containing 2.4 mM $BaCl_2$ and 2.5 nM nicked DT or reticulocyte lysates containing in vitro translated constructs to a final concentration of 2.5 nM or reticulocyte lysate where no RNA was added (''empty'' lysate). The cells were then washed extensively and bathed in Krebs-Ringer solution containing 2.4 mM $BaCl_2$ before recording. The holding potential was −40 mV and the membrane potential was shifted in 20 mV steps of 200 msec duration between −100 and +40 mV. The resulting current at the end of each voltage step was measured and plotted *vs.* the membrane potential. *I/V* curves were taken before and ~10 sec after starting ejection of gluconate buffer, pH 4.5 from a micropipette aimed directly at the cell. *(A) I/V* relationships before ejection of gluconate buffer pH 4.5 (□) and after ejection to cells exposed to ''empty'' lysate (▼), DT-B (●), DT-B E327Q (♦), DT-B D352N (★) and DT-B E362K (▲). *(B) I/V* relationships before ejection of gluconate buffer pH 4.5 (□) and after ejection to cells exposed to ''empty'' lysate (▼), DT-AB (●), DT-B D318K (♦), DT-B D295K (★) and DT-B E352K (▲). For the *I/V* relationship before ejection of low pH solution, the values from all cells recorded were averaged ($n = 53$); The data points for the different constructs represent mean values taken from 4–8 individual recordings (*cf.* Table 1).

Figure 4 shows single channel *I/V* plots derived from the recordings partially depicted in Fig. 3. The *I/V* plots were linear at negative holding potentials. At potentials approaching zero, it was difficult to resolve the dimin-

Table 1. Conductance changes induced in Vero cells exposed to DT and mutants

	Δg_m (pS)	*n*
''Empty'' lysate	5.0 ± 90.2	8
DT-AB	1,767 ± 523	6
DT-B	14,734 ± 7,303	6
DT-B D295K	269.8 ± 65.0	5
DT-B D318K	2,046 ± 534	6
DT-B E327Q	13,539 ± 8,610	6
DT-B D352N	8,313 ± 2,049	4
DT-B D352K	608.5 ± 130.4	6
DT-B E362K	11,136 ± 1,242	6

Mean values ± SD from *n* cells as indicated in the right column are shown.

ishing single-channel currents of the DT channels, due to the increased channel current of the endogenous K^+ channels. However, the *I/V* plots of the DT channels were intersecting the abscissa at potentials around 0 mV when extrapolated. The single-channel conductances, g_{sc}, calculated from the slope of the *I/V* relationships were 30–40 pS (Table 2). This agrees well with our previous estimate of 30.2 ± 11.9 pS for the single channel conductance of DT-AB [9]. Surprisingly, there was not any significant difference in g_{sc} between DT-AB, DT-B and the three mutants, although large differences were found in the whole cell recordings.

Figure 3 shows that the gating kinetics during bursts were quite different for the various toxin proteins. Moreover, there were also considerable differences in the interburst intervals, i.e., how much time the channels spent in the closed position. To quantify these differences, we determined the probabilities of the channels of being open (p(open)) and the mean dwell time in the open position. Combined with p(open), the mean dwell time characterizes the flickering kinetics, i.e., the frequency of transitions between the closed and open state during a burst. The data are summarized in Table 2. DT-B and DT-B E362K displayed a significantly higher p(open) than DT-AB and DT-B D318K. The mean dwell times for these two latter channels were similar and significantly shorter than for DT-B and DT-B E362K. In fact, DT-AB and DT-B D318K displayed quite similar Δg_m, p(open) and dwell time. All these parameters were larger for DT-B and DT-B E362K. Compared with DT-AB, the mean dwell time of DT-B D295K was less than half. P(open) was not determined for DT-B D295K because of its transient activity.

Discussion

The striking difference in channel conductances of 10 pS and 30 pS in artificial membranes *vs.* Vero cell membranes raised our concern about the possibility of DT activating an endogenous channel in Vero cells (*see* Introduction). This possibility can, however, most likely be excluded if defined mutations in the putative channel forming domain of DT have specific effects on channel properties. Our present data show that replacements of single amino acids distributed throughout a large part of the T-domain strongly affect the overall channel activity expressed as Δg_m and the gating kinetics of single channels. Thus, we conclude that the channel activity observed in DT-exposed cells at low pH [9] is inherent to DT itself and not due to DT-activation of an endogenous channel in the Vero cell membrane.

In Vero cells, the DT-B mutants varied in their ability to increase the whole-cell conductance, g_m. DT-B E327Q, DT-B D352N and DT-B E362K resembled wild-type DT-B, whereas DT-AB, DT-B D295K, DT-B D318K and DT-B D352K had a reduced Δg_m. This general pattern correlates roughly with the previously published data where channel activity in Vero cells was determined by measuring ion flux [10, 26, 29]. In these studies, however, it was not possible to detect any ion flux induced by the mutants DT-B D295K and DT-B D352K. With the high sensitivity of the patch-clamp technique, we were able to detect small, albeit significant differences in g_m induced by those mutants. The mutant D352N was reported to be less efficient than wild-type in inducing $^{86}Rb^+$-efflux in Vero cells, although it had wild-type cytotoxicity [26]. We found here that the Δg_m of DT-B D352N was the same as for the wild type. In general, the mutants which we found to induce reduced Δg_m, are also known to be less cytotoxic than the wild-type toxin when combined with fragment A [10, 26]. We observed in the present study that DT-AB induced a ~10-fold lower conductance increase, Δg_m, than DT-B at the same concentration. This difference can be partly explained by the 5–10 times lower receptor binding affinity of DT-AB [15]. But we also found differences in the gating kinetics, i.e., DT-AB exhibited significantly lower p(open) and dwell time. Hence, the presence of fragment A not only decreases the affinity to the receptor, but also apparently impedes the activity of the channel formed by fragment B, causing the channel to spend more time in its closed position. Earlier studies on ion channel formation by DT have also shown that the mutant toxin B-36 (corresponding to fragment B) is much more effective than the full length toxin (DT-AB) in inducing $^{22}Na^+$ flux in Vero cell membranes [29].

The single-channel properties of the DT-B mutants used in this study have previously been characterized in artificial membranes [17, 18, 26, 27]. Comparisons can therefore be made between effects of mutations on channel properties in artificial membrane *vs.* cell membrane. The analysis in Vero cells revealed that the mutants did not significantly differ in their single-channel conduc-

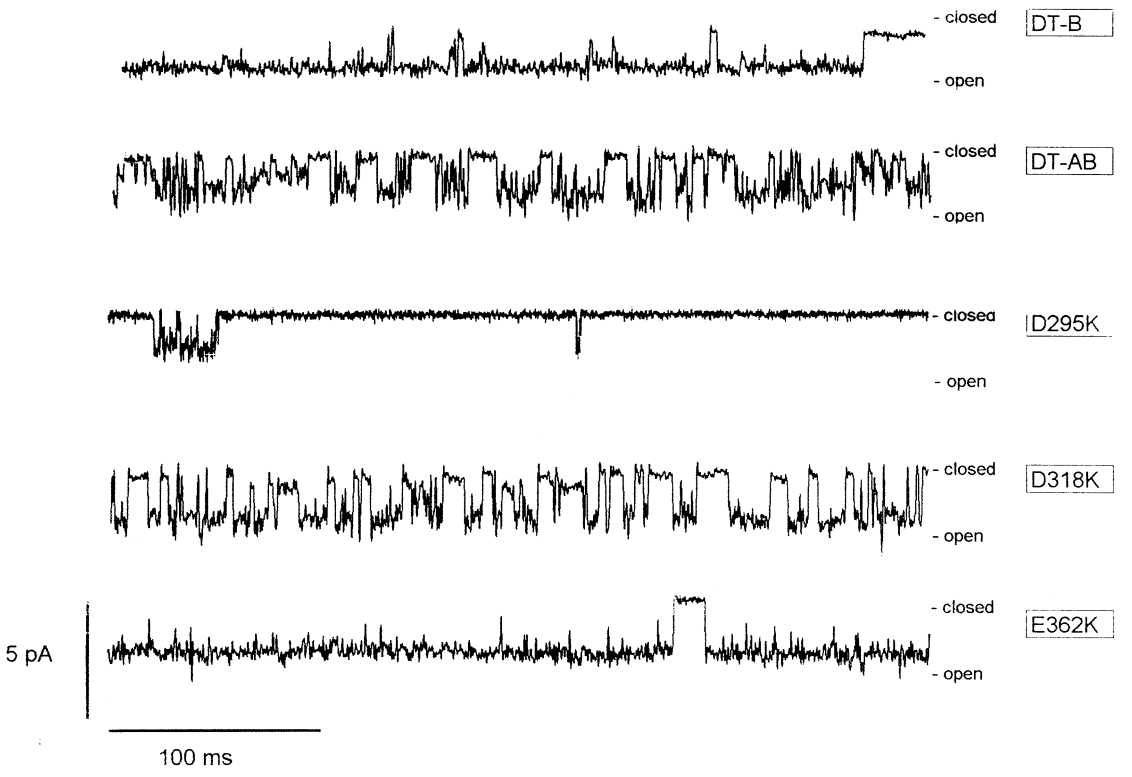

Fig. 3. Single channel recordings from DT and mutants. Vero cells were incubated for 20 min at 20°C in Krebs-Ringer solution containing 0.5 μg/ml nicked DT or reticulocyte lysates containing in vitro translated constructs to a final concentration of 2.5 nM. The cells were washed extensively and then bathed in Krebs-Ringer solution. Outside-out patches were excised and exposed to gluconate buffer, pH 4.5, by placing the patches into a stream of gluconate buffer from a large pipette (tip diameter ~5 μm). Representative traces of burst activity are shown for DT-B, DT-AB and the mutants as indicated in the figure. The holding potential was −80 mV.

tance, which was 30–40 pS. This is in conflict with data from artificial membranes, where both mutations at D318 and E362 resulted in lower conductances [17]. We found, however, that DT-B D318K and DT-B D295K displayed a lower open probability and dwell time. Glutamate at position 362 has been shown to be titratable from either side of a planar bilayer membrane and exchanging it with uncharged residues reduced the single channel conductance [17]. Therefore, it was concluded that Glu 362 lines the channel lumen at about halfway across the membrane. Here we have used a mutant where Glu 362 was exchanged with lysine, and we did not find any reduction in whole-cell current or single-channel conductance. The channel had a very high open probability and the longest dwell time of all channels tested. The mutant toxin displayed wild-type toxicity [10]. If E362 points into the channel pore, the introduced positive charge of lysine would be expected to electrostatically hinder cation flux. Reversing the charge of residues lining an ion channel can alter the ion selectivity without reducing conductance [4]. However, it is not likely that this was the case for DT-B E362K, since the reversal potential of the DT-B E362K-induced current was not changed. Moreover, it has previously been

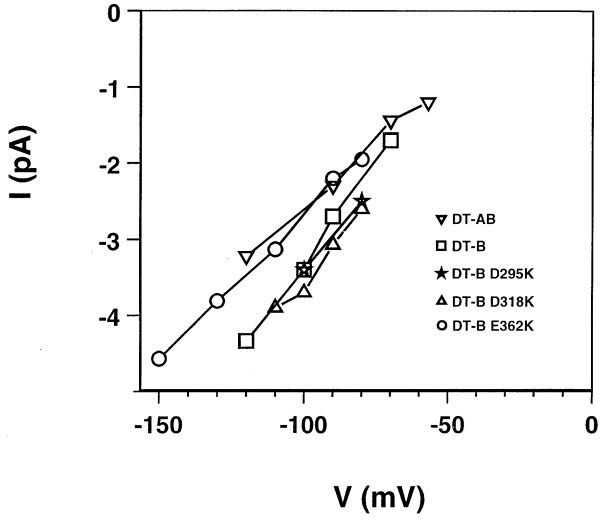

Fig. 4. *I/V* relationships of single channels. Outside-out patches excised from Vero cells exposed to DT and mutants were exposed to gluconate buffer, pH 4.5, and held at various holding potentials. The single channel currents were then plotted *vs.* the holding potential. (▽) DT-AB, (□) DT-B, (☆) DT-B D295K, (△) DT-B D318K, (○) DT-B E362K.

Table 2. Single channel properties of DT and mutants

	g_{sc} (pS)	p(open)	Mean dwell time (msec)
DT-AB	31.1 ± 5.2 (5)	0.17 ± 0.07 (3)	8.9 ± 2.5 (4)
DT-B	35.7 ± 2.6 (3)	0.45 ± 0.13 (3)	76.0 ± 36 (3)
DT-B D295K	36.0 (2)	n.d.	3.5 (2)
DT-B D318K	34.2 ± 13.7 (3)	0.21 ± 0.06 (3)	11.7 ± 1.1 (3)
DT-B E362K	41.1 ± 8.0 (4)	0.80 ± 0.1 (3)	165.7 ± 58 (3)

Mean values ± SD are shown. The number in brackets indicates the number of recordings. There was no voltage dependency of p(open) and mean dwell time within the voltage range where the DT channels were observed (*data not shown*). All the values for p(open) and mean dwell time were determined at a holding potential of −80 mV.

shown that DT-B E362K induces $^{22}Na^{+}$ influx into Vero cells to the same extent as DT-B [10].

An important finding in this work is that mutations of negatively charged amino acids in the DT B-fragment have effects on channel activity in Vero cells distinct from those reported in artificial membranes, suggesting that the channel may have a different structure in the Vero cell membrane. Also, the replacement of the transmembrane and intracellular domains of the DT receptor with a GPI-anchor abrogates channel formation while toxin binding and A-fragment translocation is intact [14], indicating that the DT receptor may also be involved in channel formation. Thus, the channel observed in the plasma membrane of Vero cells may be the result of a complex interaction between the B-fragment, the DT receptor, and possibly other cellular proteins.

This work was supported by the Norwegian Research Council, by the Norwegian Cancer Society, by the Jahre Foundation, by the Family Blix legacy, by the Otto and Rachel Bruun's legacy and by the Novo Nordisk Fund. M.L. had a research grant from the Norwegian Research Council and the EU program ''Human Capital and Mobility.''

References

1. Ahmad, I., Korbmacher, C., Segal, A.S., Cheung, P., Boulpaep, E.L., Barnstable, C.J. 1992. Mouse cortical collecting duct cells show nonselective cation channel activity and express a gene related to the cGMP-gated rod photoreceptor channel. *Proc. Natl. Acad. Sci. USA* **89:**10262–10266
2. Bennett, M.J., Choe, S., Eisenberg, D. 1994. Refined structure of dimeric diphtheria toxin at 2.0 A resolution. *Protein Sci.* **3:**1444–1463
3. Bennett, M.J., Eisenberg, D. 1994. Refined structure of monomeric diphtheria toxin at 2.3 A resolution. *Protein Sci.* **3:**1464–1475
4. Blachly-Dyson, E., Songzhi, P., Colombini, M., Forte, M. 1990. Selectivity Changes in Site-Directed Mutants of the VDAC Ion Channel: Structural Implications. *Science* **247:**1233–1236
5. Choe, S., Bennett, M.J., Fujii, G., Curmi, P.M., Kantardjieff, K.A., Collier, R.J., Eisenberg, D. 1992. The crystal structure of diphtheria toxin. *Nature* **357:**216–222
6. Collier, R.J. 1975. Diphtheria toxin: mode of action and structure. *Bacteriol. Rev.* **39:**54–85
7. Dietl, P., Volkl, H. 1994. Maitotoxin activates a nonselective cation channel and stimulates Ca^{2+} entry in MDCK renal epithelial cells. *Mol. Pharmacol.* **45:**300–305
8. Donovan, J.J., Simon, M.I., Draper, R.K., Montal, M. 1981. Diphtheria toxin forms transmembrane channels in planar lipid bilayers. *Proc. Natl. Acad. Sci. USA* **78:**172–176
9. Eriksen, S., Olsnes, S., Sandvig, K., Sand, O. 1994. Diphtheria toxin at low pH depolarizes the membrane, increases the membrane conductance and induces a new type of ion channel in Vero cells. *EMBO J.* **13:**4433–4439
10. Falnes, P.Ø., Madshus, I.H., Sandvig, K., Olsnes, S. 1992. Replacement of negative by positive charges in the presumed membrane-inserted part of diphtheria toxin B fragment. Effect on membrane translocation and on formation of cation channels. *J. Biol. Chem.* **267:**12284–12290
11. Greenfield, L., Bjorn, M.J., Horn, G., Fong, D., Buck, G.A., Collier, R.J., Kaplan, D.A. 1983. Nucleotide sequence of the structural gene for diphtheria toxin carried by corynebacteriophage beta. *Proc. Natl. Acad. Sci. USA* **80:**6853–6857
12. Hamill, O.P., Marty, A., Neher, E., Sakmann, B., Sigworth, F.J. 1981. Improved patch-clamp techniques for high-resolution current recording from cells and cell-free membrane patches. *Pfluegers Arch.* **391:**85–100
13. Kagan, B.L., Finkelstein, A., Colombini, M. 1981. Diphtheria toxin fragment forms large pores in phospholipid bilayer membranes. *Proc. Natl. Acad. Sci. USA* **78:**4950–4954
14. Lanzrein, M., Sand, O., Olsnes, S. 1996. GPI-anchored diphtheria toxin receptor allows membrane translocation of the toxin without detectable ion channel activity. *EMBO J.* **15:**725–734
15. McGill, S., Stenmark, H., Sandvig, K., Olsnes, S. 1989. Membrane interactions of diphtheria toxin analyzed using in vitro synthesized mutants. *EMBO J.* **8:**2843–2848
16. Merot, J., Bidet, M., Gachot, B., Le Maout, S., Tauc, M., Poujeol, P. 1988. Patch clamp study on primary culture of isolated proximal convoluted tubules. *Pfluegers Arch.* **413:**51–61
17. Mindell, J.A., Silverman, J.A., Collier, R.J., Finkelstein, A. 1994. Structure-function relationships in diphtheria toxin channels: III. Residues which affect the cis pH dependence of channel conductance. *J. Membrane Biol.* **137:**45–57
18. Mindell, J.A., Silverman, J.A., Collier, R.J., Finkelstein, A. 1994. Structure function relationships in diphtheria toxin channels: II. A residue responsible for the channel's dependence on trans pH. *J. Membrane Biol.* **137:**29–44
19. Mindell, J.A., Zhan, H., Huynh, P.D., Collier, R.J., Finkelstein, A. 1994. Reaction of diphtheria toxin channels with sulfhydryl-specific reagents: observation of chemical reactions at the single molecule level. *Proc. Natl. Acad. Sci. USA* **91:**5272–5276
20. Montecucco, C., Papini, E. 1995. Cell penetration of bacterial protein toxins. *Trends Microbiol.* **3:**165–167
21. Olsnes, S., van Deurs, B., Sandvig, K. 1993. Protein toxins acting on intracellular targets: cellular uptake and translocation to the cytosol. *Med. Microbiol. Immunol.* **182:**51–61
22. Papini, E., Sandona, D., Rappuoli, R., Montecucco, C. 1988. On the membrane translocation of diphtheria toxin: at low pH the toxin induces ion channels on cells. *EMBO J.* **7:**3353–3359
23. Pappenheimer, A.M., Jr. 1977. Diphtheria toxin. *Annu. Rev. Biochem.* **46:**69–94
24. Paulais, M., Teulon, J. 1989. A cation channel in the thick ascending limb of Henle's loop of the mouse kidney: inhibition by adenine nucleotides. *J. Physiol.* **413:**315–327
25. Sandvig, K., Olsnes, S. 1988. Diphtheria toxin-induced channels in

Vero cells selective for monovalent cations. *J. Biol. Chem.* **263:**12352–12359

26. Silverman, J.A., Mindell, J.A., Finkelstein, A., Shen, W.H., Collier, R.J. 1994. Mutational analysis of the helical hairpin region of diphtheria toxin transmembrane domain. *J. Biol. Chem.* **269:** 22524–22532
27. Silverman, J.A., Mindell, J.A., Zhan, H., Finkelstein, A., Collier, R.J. 1994. Structure-function relationships in diphtheria toxin channels: I. Determining a minimal channel-forming domain. *J. Membrane Biol.* **137:**17–28
28. Stenmark, H., Afanasiev, B.N., Ariansen, S., Olsnes, S. 1992. Association between diphtheria toxin A- and B-fragment and their fusion proteins. *Biochem. J.* **281:**619–625
29. Stenmark, H., McGill, S., Olsnes, S., Sandvig, K. 1989. Permeabilization of the plasma membrane by deletion mutants of diphtheria toxin. *EMBO J.* **8:**2849–2853
30. Teulon, J., Paulais, M., Boutheir, M. 1987. A Ca2-activated cation-selective channel in the basolateral membrane of the cortical thick ascending limb of Henle's loop of the mouse. *Biochim. Biophys. Acta* **905:**125–132
31. Yamaizumi, M., Mekada, E., Uchida, T., Okada, Y. 1978. One molecule of diphtheria toxin fragment A introduced into a cell can kill the cell. *Cell* **15:**245–250
32. Zhan, H., Choe, S., Huynh, P.D., Finkelstein, A., Eisenberg, D., Collier, R.J. 1994. Dynamic transitions of the transmembrane domain of diphtheria toxin: Disulfide trapping and fluorescence proximity studies. *Biochemistry* **33:**11254–11263